Environmental Research 279 (2025) 121797

Contents lists available at ScienceDirect

Environmental Research

journal homepage: www.elsevier.com/locate/envres

Effects of phthalate exposure on human ovarian extracellular matrix composition: insights from a 3D spheroid model

Saba Nikanfar [a], Ellen C.R. Leonel [b,c], Pauliina Damdimopoulou [d,e], Jodi A. Flaws [f], Christiani A. Amorim [a,*]

[a] Pôle de Recherche en Physiopathologie de la Reproduction, Institut de Recherche Expérimentale et Clinique, Université Catholique de Louvain, Brussels, Belgium
[b] Animal Molecular and Cellular Biology Group, Louvain Institute of Biomolecular Science and Technology, Université catholique de Louvain, Louvain-la-Neuve, Belgium
[c] Institute of Biological Sciences, Federal University of Goiás, Goiânia, Brazil
[d] Division of Obstetrics and Gynecology, Department of Clinical Science, Intervention and Technology, Karolinska Institutet and Karolinska University Hospital, Stockholm, Sweden
[e] Department of Gynecology and Reproductive Medicine, Karolinska University Hospital, Stockholm, Sweden
[f] Department of Comparative Biosciences, University of Illinois at Urbana-Champaign, United States

ARTICLE INFO

Keywords:
Extracellular matrix
Ovarian ECM toxicity
Phthalate exposure
Spheroids

ABSTRACT

Phthalates, widely used as plasticizers in consumer products, have become a significant public health concern due to their toxic effects on reproductive and endocrine systems. However, the specific mechanisms by which phthalates affect ovarian function remain poorly understood. To address this knowledge gap, we employed 3D spheroids derived from human ovarian stromal cells, which mimic the ovarian tissue. Since remodeling the ovarian extracellular matrix (ECM) is centrally involved in follicle growth, ovulation, and ovarian aging, we decided to study the impact of environmentally relevant phthalate mixtures (PM) on ECM components. Spheroids were generated from both reproductive-aged and menopausal ovarian tissues, then treated with PM for four days. Collagen deposition was assessed using picrosirius red staining, while immunofluorescence was used to evaluate the proliferation and deposition of collagen type VI, elastin, fibrillin-1, and elastin microfibril interfacer 1 (EMILIN-1). Our results revealed that PM exposure significantly increased collagen deposition ($p < 0.0001$) in spheroids from reproductive-aged ovaries, while reducing collagen VI levels ($p < 0.05$), potentially compromising the structural and functional integrity of the ovarian ECM. In contrast, spheroids from menopausal ovaries exhibited a decrease in EMILIN-1 ($p < 0.05$) and fibrillin-1 ($p < 0.001$), both crucial for maintaining tissue elasticity. These findings underscore the detrimental effects of phthalates on ovarian ECM across different age groups, with a particular emphasis on ECM elastisity. Additionally, this study highlights the utility of 3D spheroids as a reliable in vitro model for mechanistic research, drug screening and toxicology testing.

1. Introduction

Phthalates, widely used as plasticizers to improve polymer flexibility in various consumer products, have become a significant public health concern because of their well-documented toxic effects on reproductive and endocrine systems (Kavlock et al., 2002). Given the weak molecular bonds between phthalates and polymers, these chemicals are easily released into the environment, entering the human body through multiple routes such as inhalation, ingestion, and skin absorption (Bergé et al., 2013; Hongjun et al., 2013; Martine et al., 2013). Additionally, as integral components of plastics, phthalates can enter our bodies through nano- and microplastics (Hong et al., 2023). While extensive research has focused on the effects of single phthalates, human exposure often involves mixtures of these chemicals, making it crucial to study phthalate mixtures (PM) to better understand their combined impact, particularly on female reproductive health. Additionally, the precise mechanisms through which phthalates exert their adverse effects on reproductive function remain poorly understood, despite recent efforts to identify these mechanisms via transcriptomics (Mattson and Warner, 2025; Tarvainen et al., 2023; Visser et al., 2024). The dynamic role of the extracellular matrix (ECM) in the ovary is crucial for folliculogenesis as it undergoes significant changes to support and regulate intricate

* Corresponding author. Pôle de Recherche en Physiopathologie de la Reproduction, Institut de Recherche Expérimentale et Clinique, Université Catholique de Louvain, Avenue Hippocrate 54, Bte B1.55.03, 1200, Brussels, Belgium.
E-mail address: christiani.amorim@uclouvain.be (C.A. Amorim).

https://doi.org/10.1016/j.envres.2025.121797
Received 4 March 2025; Received in revised form 2 May 2025; Accepted 5 May 2025
Available online 7 May 2025

cellular reorganization within developing follicles. Recent studies have highlighted that ovary is a mechano-responsive organ, with crosstalk between the ECM, follicles, and ovarian cells being vital for successful folliculogenesis and oogenesis (Ouni et al., 2021).

During human follicle activation, a decrease in the ratio of thicker to thinner collagen fibers has been observed. As follicles grow, there is a reduction in elastin content, along with decreased levels of fibrillin-1 and EMILIN-1 (Ouni et al., 2020). Besides these changes, the aging process also leads to a denser and more compact ECM structure. Collagens I and III levels increase, while elastin content declines (Dipali et al., 2023). Furthermore, downregulation of fibrillin-2 has been observed with aging in the mouse ovary, further emphasizing the impact of aging on ECM composition and its implications for ovarian function.

Evidence has shown that exposure to phthalate mixtures can impair antral follicle growth, cause oocyte fragmentation, and disrupt steroidogenic enzyme activity (Tarvainen et al., 2023). Numerous studies have investigated the effects of individual phthalates, particularly di (2-ethylhexyl) phthalate (DEHP), on ovarian cells, often using short-term in vitro models and relatively high concentrations (1–50,000 μM) (Evangelinakis et al., 2024; Varik et al., 2024). These studies consistently report reduced cell viability, increased apoptosis, and in some cases, elevated oxidative stress, suggesting a direct cytotoxic impact on ovarian cells (Adir et al., 2017; Chang et al., 2017; Chen et al., 2012). More recent research has shifted toward evaluating phthalate mixtures, which more accurately reflect real-life environmental exposures. These mixture-based studies, conducted across a wide concentration range (0.065–1000 μg/mL) and over longer exposure durations, have demonstrated oxidative stress induction, impaired antral follicle development, increased follicular atresia, and reduced ovulation rates (Land et al., 2021; Meling et al., 2020; Rasmussen et al., 2017; Zhou and Flaws, 2017). In vivo animal models corroborate these findings, showing phthalate-induced apoptosis, altered follicle dynamics, and disruptions in ovarian steroidogenesis, including altered levels of FSH, LH, and testosterone (Safar et al., 2023). Additionally, phthalate mixtures have been shown to affect gene and microRNA expression patterns involved in cell cycle regulation, steroid biosynthesis, and oocyte maturation (Barnett-Itzhaki et al., 2021). Of particular concern are prenatal and gestational exposures, which have been linked to impaired folliculogenesis, an increase in primordial and atretic follicles, and disruptions in hormonal signaling (Repouskou et al., 2019). These developmental exposures can have long-lasting effects, as evidenced by multigenerational rodent studies demonstrating impaired folliculogenesis and steroidogenesis in both F1 and F2 generations (Gonsioroski et al., 2022).

These findings suggest that phthalate exposures, whether individual, combined, or occurring during critical windows of development, pose a significant risk to ovarian function and may contribute to reproductive disorders, including polycystic ovary syndrome (Zhang et al., 2023).

However, the exact cellular processes and pathways affected by these exposures remain insufficiently understood. Given the widespread use of phthalates, which have been detected in numerous biological samples such as urine, serum, saliva, breast milk, and follicular fluid (FF) (Du et al., 2016; Krotz et al., 2012; Bellavia et al., 2023), there is an urgent need for sensitive and validated in vitro models for reproductive toxicology studies.

In this study, we bridged these knowledge gaps by employing spheroids as 3D models to investigate the effects of environmentally relevant PMs on ovarian ECM components, which are essential for ovarian function and fertility. By focusing on mixtures, using advanced 3D models, and examining less-studied effects on ECM components, our research seeks to provide a more comprehensive understanding of phthalate-induced reproductive toxicity in females, contributing to improved regulatory and safety assessment protocols for these ubiquitous environmental contaminants.

2. Materials and methods

2.1. Ovarian tissue collection

Ovarian tissue biopsies were obtained from two groups including four healthy reproductive-aged (21–49 years old) and four menopausal women (64–68 years old). The study was approved by the Institutional Review Board of the Université Catholique de Louvain (IRB reference 2018/19DEC/475 for menopausal multi-organ donors and IRB reference 2012/23MAR/125 and 2018/19DEC/475 for reproductive-aged women). Upon collection, both types of tissue were immediately transported to the laboratory in Dulbecco's phosphate-buffered saline (DPBS) (Gibco, Thermo Fisher Scientific, Merelbeke, Belgium) at 4 °C. The medullary part of the ovary was then removed, and the cortical region was selected for subsequent experiments, as it contains the majority of follicles and is the primary site of stromal remodeling in response to environmental exposures. Then cortex was cut into 5x5x1 mm sections and frozen following standard procedures (Gallardo et al., 2018).

Fig. 8 provides an overview of the workflow and summarizes the different experiments performed throughout the study.

2.2. Ovarian stromal cell isolation

After thawing, ovarian stromal cells were isolated using a protocol that involved both mechanical and enzymatic methods (Chiti et al., 2017). The tissue was first mechanically minced using a tissue chopper (Mickel Laboratory, Guildford, UK) and then enzymatically digested with Liberase DH (Sigma-Aldrich, Darmstadt, Germany) and DNase I (Sigma-Aldrich) at 37 °C for 75 min. The enzymatic reaction was stopped by adding DPBS supplemented with 10 % heat-inactivated fetal bovine serum (FBS) (Gibco). The resulting cell suspension was filtered through 80 μm and 20 μm nylon net filters (Millipore, Overijse, Belgium) and centrifuged at 500 g for 10 min. The pellet was resuspended in Dulbecco's modified Eagle's medium F-12 (DMEM/F12; Gibco) supplemented with 10 % FBS and 1 % antibiotic-antimycotic (Gibco).

2.3. Spheroid formation

After cell counting, 100,000 stromal cells isolated from the ovarian cortex of each individual donor were seeded into separate agarose-based microwell molds (MicroTissues, Inc., Providence, RI, USA) in DMEM/F12 supplemented with 10 % FBS and 1 % antibiotic-antimycotic, allowing the formation of up to 98 spheroids per mold. To ensure spatial representation of the ovarian tissue, stromal cells were extracted from three distinct regions of the cortex for each donor, pooled into a single-cell suspension, and used for spheroid formation. Importantly, cells from different donors were not pooled at any stage. All spheroids derived from a single donor were treated and analyzed independently, with experimental groups composed of four biological replicates ($n = 4$ per group). While multiple spheroids were generated per donor, these were considered technical replicates and used to ensure reproducibility within each individual sample. Statistical analysis was conducted using the donor (ovary) as the experimental unit. The cultures were incubated at 37 °C with 5 % CO_2 for three days, after which the culture medium was replaced every other day for another three days.

2.4. Treatments

Treatments began on day 6 and continued for four days. The PM was formulated based on the concentrations of different phthalate components, including mono(2-ethyl-5-hydroxyhexyl) phthalate 8.1 %, racemic mono(ethylhexyl) phthalate 1.3 %, mono(2-ethyl-5-oxyhexyl) phthalate 3.1 %, racemic mono(5-carboxy-2ethylpentyl) phthalate 6.4 %, monoisobutyl phthalate 5.3 %, monobenzyl phthalate 2.6 %, mono (3-carboxypropyl) phthalate 0.8 %, monoethyl phthalate 65.6 %, and monobutyl phthalate 6.7 % as measured in urine samples from the

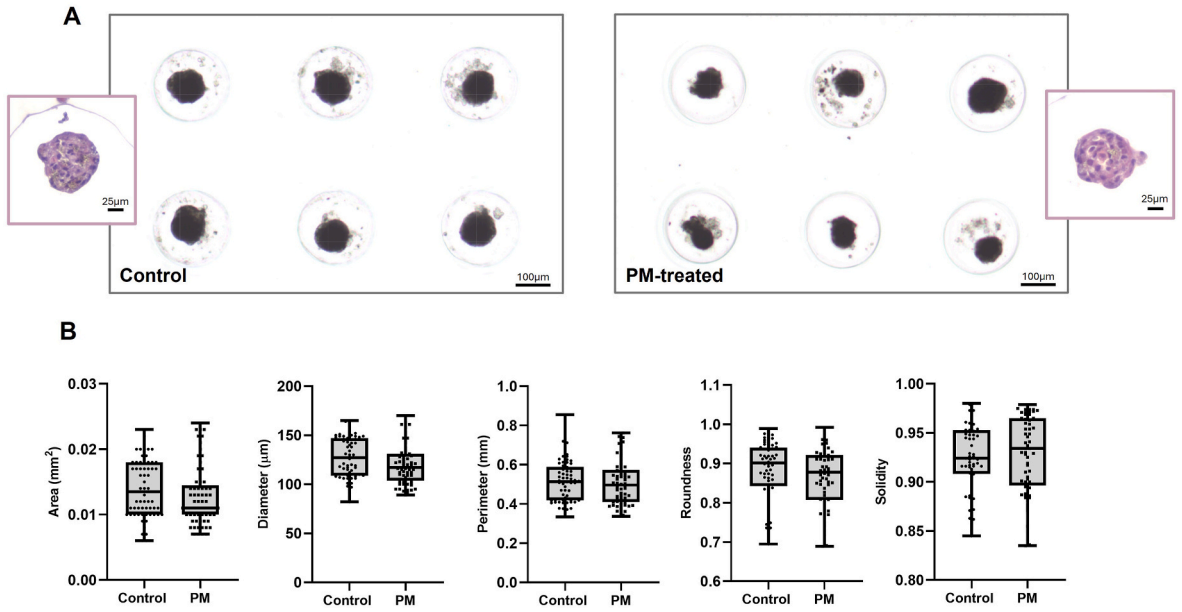

Fig. 1. Microscopic images (A) and morphological analysis (B) of spheroids derived from reproductive-aged ovaries following treatment for four days with a phthalate mixture (PM) compared to the control group. All values are presented as the median ± interquartile range (IQR) of 60 spheroids per group.

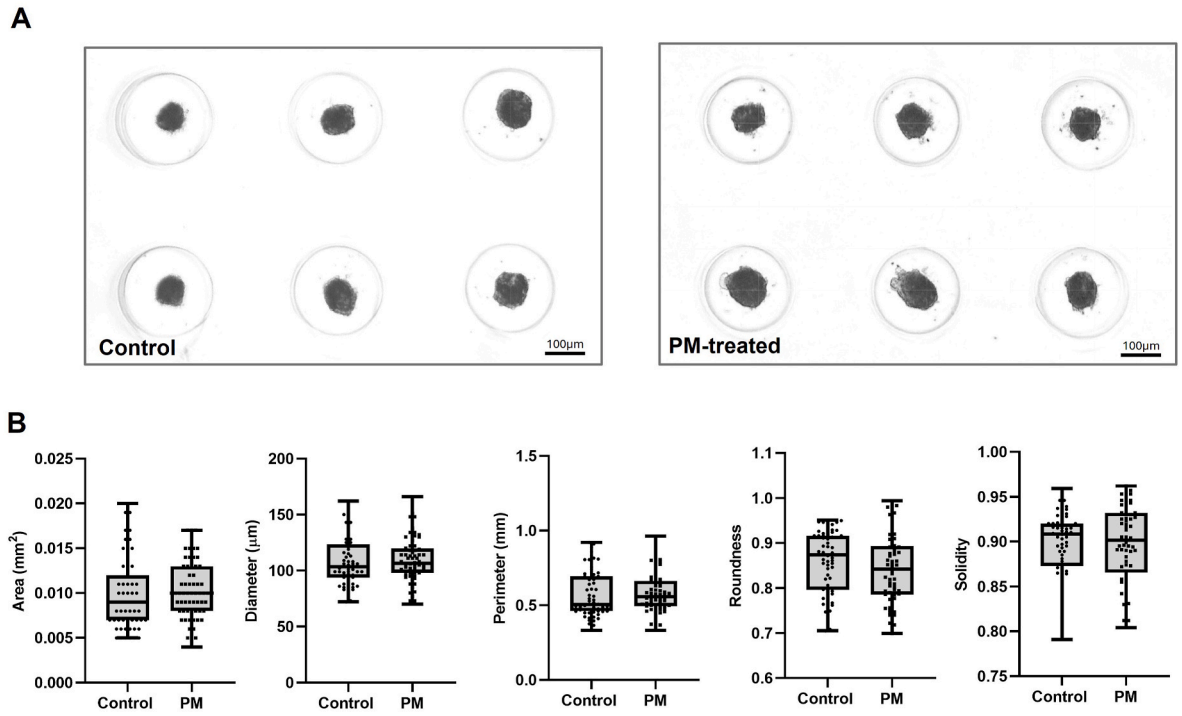

Fig. 2. Microscopic images (A) and morphological analysis (B) of spheroids derived from menopausal ovaries following treatment for four days with a phthalate mixture (PM) compared to the control group. All values are presented as the median ± interquartile range (IQR) of 60 spheroids per group.

midlife woman's health cohort study (MWHS) (Tarvainen et al., 2023). Previous studies showed no cytotoxicity induced by the 1x and 100x PM in human and mouse ovarian cell models (Tarvainen et al., 2023). Therefore, the 100x concentration was selected to capture the full range of potential effects. Spheroids generated from each patient were divided into two experimental groups: one group was treated with PM, added to the medium at a concentration of 0.75 μL/ml of the mixture stock to reach a final concentration of 200 μM while the other served as the control group consisting of DMSO (0.075 %). The medium was renewed daily. Morphological features of the spheroids were measured on days 6 (start of treatment) and 10 (end of treatment) using an inverted microscope to assess development. After generating binary masks to separate the spheroid mass from the image background, morphological analysis was conducted using the Analyze Particles function in ImageJ/Fiji software (ImageJ 1.54f; National Institutes of Health, USA). This function was used to quantify various morphological features of the spheroids, including diameter, perimeter, area, solidity (area/convex area), and roundness $(4 \times \text{area}/(\pi \times \text{major axis}))^2$.

On day 10, the spheroids were fixed in 4 % paraformaldehyde overnight at 4 °C and then embedded in HistoGel (Thermo Scientific),

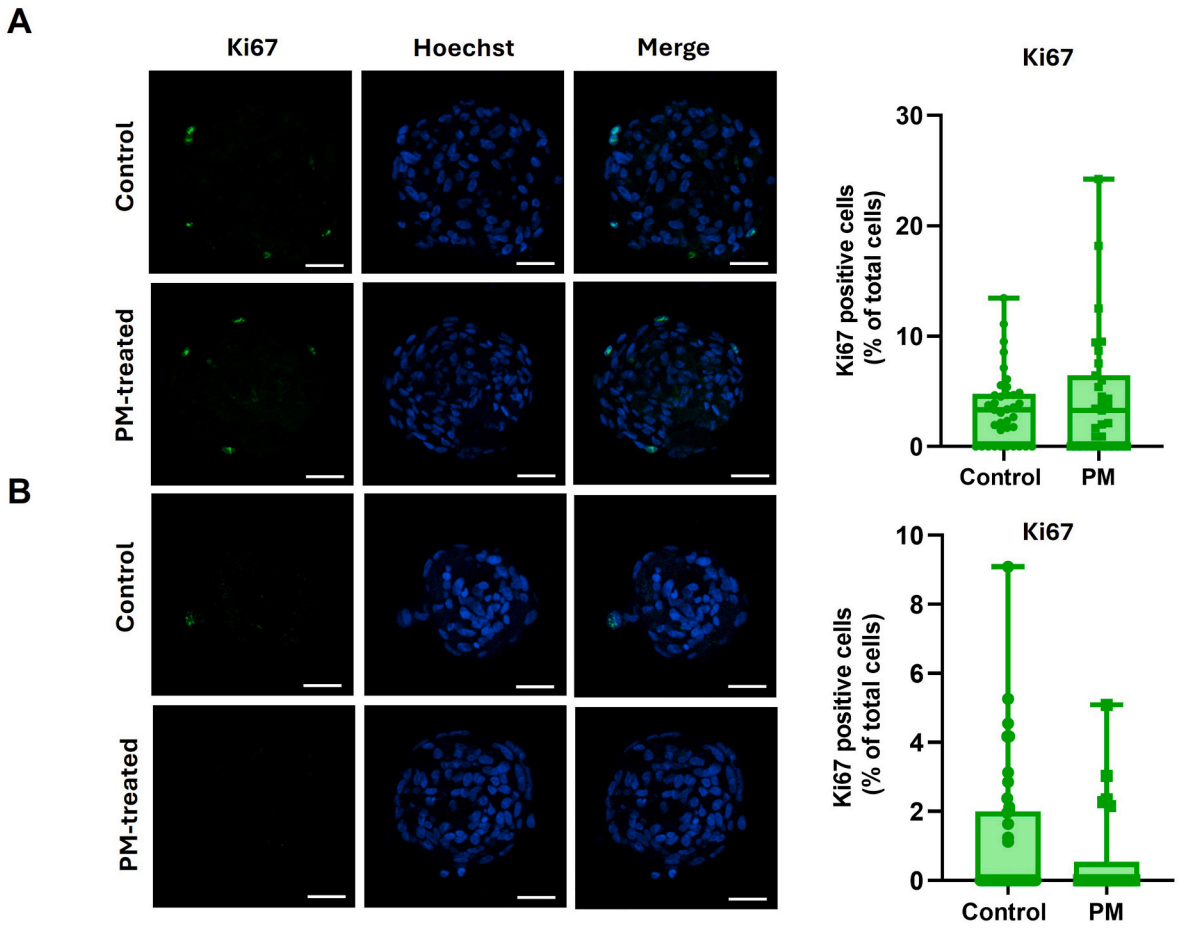

Fig. 3. Ki67 immunofluorescence staining images and quantification of Ki67-positive cells of spheroids isolated from reproductive-age (A) and menopausal ovaries (B) treated with PM for four days. The quantification of Ki67-positive cells is presented as box plots, with median values indicated by lines. Altogether 131 spheroids were quantified. White bars indicate 25 μm.

before being dehydrated and embedded in paraffin blocks.

2.5. Immunofluorescence staining

Immunofluorescence analysis was conducted on consecutive 5-μm-thick tissue sections to assess proliferation activity and ECM components of the spheroids, using antibodies against collagen type VI, elastin microfibril interfacer 1 (EMILIN-1), and fibrillin-1. Paraffin sections were first deparaffinized, followed by quenching of autofluorescence with a 10-min incubation in 50 mM NH_4Cl in PBS. Antigen retrieval was performed in a water bath containing 10 mM citrate buffer and 0.1 % Triton X-100. To block non-specific antigen-binding sites, the sections were treated with Tris-buffered saline/Tween containing 10 % normal goat serum and 1 % bovine serum albumin (BSA). The sections were then incubated overnight at 4 °C in a humid chamber with the following primary antibodies diluted in TBS containing 1 % BSA and 0.1 % Tween-20 %: monoclonal antibody of anti-Ki67 (1:90, M7240; Dako, Glostrup, Denmark), polyclonal antibodies of anti-collagen VI α3 (1:100, PAS-49914; Thermo Fisher Scientific), anti-EMILIN-1 (1:200, HPA002822; Sigma-Aldrich), and anti-fibrillin-1 (1:100, HPA017759; Sigma-Aldrich). The next day, the sections were incubated for 1 h at room temperature with Alexa Fluor 488 goat anti-mouse (1:250) for Ki67 and Alexa Fluor 488 goat anti-rabbit (1:500) for collagen VI, EMILIN-1, and fibrillin-1. Nuclei were counterstained with Hoechst 33342 (1:500, Thermo Fisher Scientific) and sections were mounted using Fluoromount™ Aqueous Mounting Medium (Sigma-Aldrich).

Human ovarian cortex was used for positive controls of tested antibodies and negative controls were prepared by omitting the primary antibodies (Supplementary Fig. S1). The stained slides were digitized using a confocal microscope (LSM800; Zeiss) equipped with a 488 nm laser line.

2.6. Picrosirius red staining

Picrosirius red staining (PSR) was used to quantify collagen content in the spheroids. For this, 5 μm-thick paraffin sections were used. These sections were deparaffinized using Histosafe (Yvsolab SA, Beerse, Belgium) and ethanol, rehydrated, and then immersed in a 3 % phosphomolybdic acid solution for 5 min to acclimate to the pH and provide yellow counterstaining. After rinsing with water, the sections were incubated for 2 h at room temperature in saturated aqueous picric acid solution containing 0.1 % Direct Red 80 (Sigma-Aldrich). The sections were then briefly washed in 0.01 N HCl for 2 min, rinsed with water, dehydrated, and mounted using a Tissue-Tek film coverslipper (Sakura, Antwerp, Belgium). Finally, images were captured using the Zeiss Axio Imager Apo Tome microscope.

2.7. Statistical analysis

Data are presented as mean ± SEM for normally distributed data and as median ± IQR for non-normally distributed data. Distributions and outliers were visualized using Tukey's box plots. For cases where the median served as the primary measure of central tendency in graphical representations, the mean was also reported for comparison purposes. All statistical calculations were performed using GraphPad Prism software package (version 8.0; San Diego, CA, USA). The distribution of

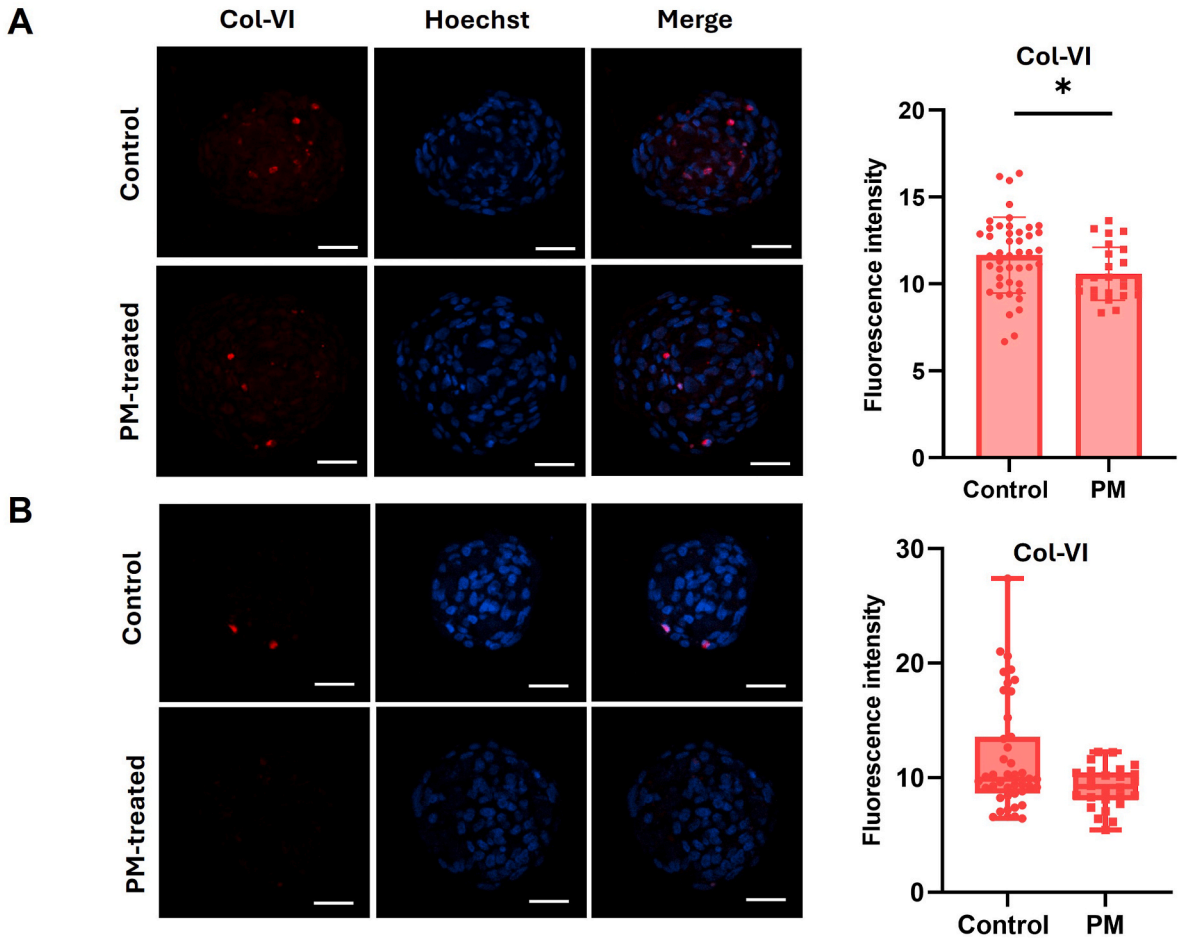

Fig. 4. Collagen VI (Col-VI) immunofluorescence staining images and quantification of Col-VI expression in spheroids isolated from reproductive-aged (A) and menopausal ovaries (B) exposed to PM for four days. Fluorescence intensities are presented as histograms (mean ± SEM) for normally distributed data and box plots (median ± IQR) for non-normally distributed data. A total of 139 spheroids were analyzed across all donors and treatment conditions. Each dot represents a single spheroid (technical replicate). Statistical analyses were performed using the average value per donor (biological replicate, n = 4 per group). The white bars indicate 25 μm * shows $p < 0.05$. Note: Due to the compact and three-dimensional structure of the spheroids, some Col-VI staining may appear perinuclear or intracellular. This is likely the result of sectioning artifacts and spatial overlap between adjacent cells, rather than true nuclear localization.

quantitative data was assessed using the Shapiro-Wilk test. The multiple Student's t-test or Mann-Whitney test was used to compare differences between the phthalate-treated and control groups. Differences were considered statistically significant at a p value < 0.05.

Each dot shown in the graphs represents a single spheroid (technical replicate). However, statistical analyses were conducted using the donor (ovary) as the experimental unit (n = 4 per group). For each donor and condition, the values from all analyzed spheroids were averaged, and these per-donor means or medians were used in statistical comparisons. This approach preserves biological independence while accounting for intra-donor variability.

3. Results

3.1. PM treatment does not affect spheroid morphology and proliferation

Figs. 1 and 2 show images of the spheroids after PM treatment for four days. In the reproductive-age group, the evaluation of spheroid diameter showed comparable sizes on day 6 between spheroids designated for PM treatment (121.6 ± 2.4 μm) and control (128.6 ± 2.6 μm) group. As illustrated in Fig. 1, by day 10, no significant differences were observed in the spheroid diameter (128.1 ± 4.217 vs. 130.7 ± 2.941 in the control), perimeter (0.539 ± 0.028 vs. 0.544 ± 0.015 in the control), area (0.0142 ± 0.0009± 0.0148 ± 0.0006 in the control), roundness (0.827 ± 0.014 vs. 0.866 ± 0.013 in the control), or solidity (0.947 ± 0.003 vs. 0.938 ± 0.002 in the control). In the menopausal group, the spheroid morphology analysis (Fig. 2) indicated that the sizes were comparable on day 6 between the spheroids designated for PM treatment (112.5 ± 1.1 μm) and control (109 ± 1.3 μm) groups. By day 10, no significant differences in spheroid size were observed between the PM-treated (107.2 ± 1.2 μm) and control (104 ± 1.2 μm) groups. Similarly, other parameters, including perimeter, area, roundness, and solidity, did not exhibit any significant changes following the treatment. Moreover, the expression of Ki67-positive cells did not demonstrate any significant difference in either the reproductive age or menopausal groups (Fig. 3).

3.2. Effects of PM treatment on ECM components

To investigate the effects of PM on ECM components, we first assessed the protein levels of collagen VI in spheroids from both experimental groups and compared them to the corresponding control groups. The results showed a significant decrease in collagen VI levels in spheroids from reproductive-aged ovaries (10.59 ± 0.30 in PM vs. 11.66 ± 0.32 in control, $p < 0.05$), while no significant changes were observed in the menopausal group (Fig. 4).

We also measured collagen levels (types I and III) by PSR staining. Interestingly, the results showed a significant increase in these collagen

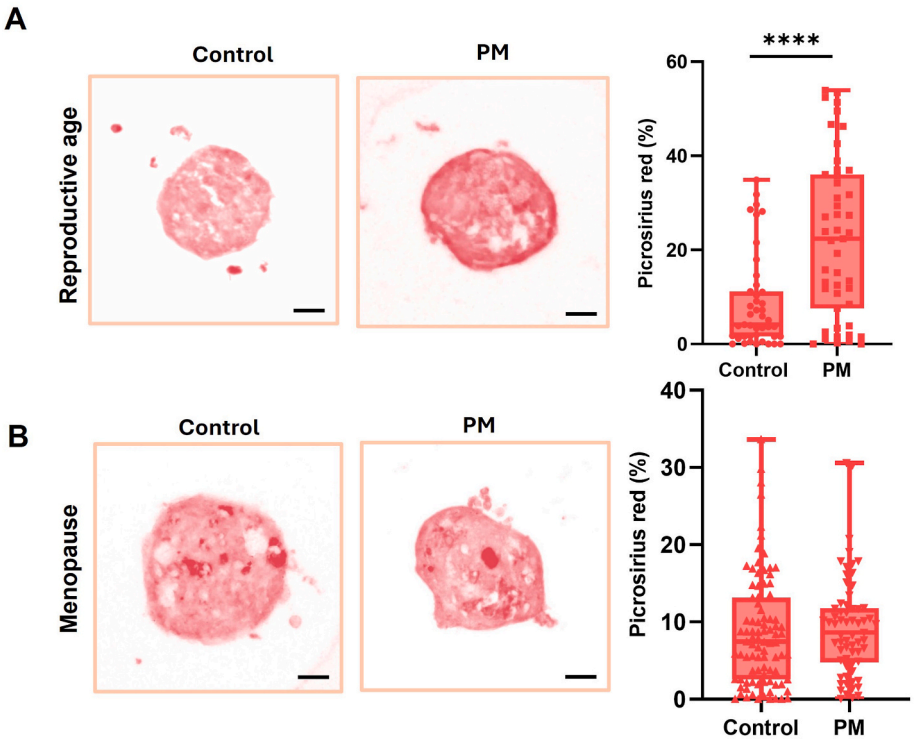

Fig. 5. Picrosirius red-stained images of the spheroids isolated from reproductive age (A) and menopausal ovaries (B) and quantification (C) exposed to PM for four days. All the values are shown as median ± IQR. A total of 245 spheroids were analyzed across all donors and treatment conditions. Each dot represents a single spheroid (technical replicate). Statistical analyses were performed using the average value per donor (biological replicate, n = 4 per group). The scale bars indicate 25 μm **** Indicates $p < 0.0001$. (For interpretation of the references to colour in this figure legend, the reader is referred to the Web version of this article.)

types in spheroids from reproductive-aged ovaries after PM treatment compared to control (22.59 ± 2.49 vs. 8.75 ± 1.53 in control, $p < 0.0001$). In contrast, collagen levels in spheroids from menopausal ovaries were not affected by PM exposure (Fig. 5).

Immunofluorescence results revealed no notable differences in EMILIN-1 levels in spheroids from reproductive-aged ovaries following PM treatment compared to control spheroids from reproductive-aged ovaries. However, PM significantly decreased EMILIN-1 levels in spheroids from menopausal ovaries compared to control spheroids from menopausal ovaries (37.93 ± 1.66 vs. 43.71 ± 1.64 in control, $p < 0.05$) (Fig. 6) .

Similarly, fibrillin-1 levels followed a pattern comparable to that of EMILIN-1 in both groups. No significant changes were observed in fibrillin-1 levels in spheroids from reproductive-aged ovaries after PM treatment compared to control spheroids from reproductive-aged women. In contrast, fibrillin-1 levels decreased significantly in spheroids from menopausal ovaries compared to control spheroids from menopausal ovaries (11.03 ± 0.48 vs. 15.00 ± 0.82, $p < 0.001$) (Fig. 7).

4. Discussion

Morphological analysis of ovarian spheroids derived from cortical cells indicated that tissue responses to PM exposure vary depending on the reproductive stage of the ovaries in the woman's life. Specifically, spheroids from reproductive-aged ovaries exhibited alterations in the ECM composition, particularly collagen types I, III, and VI, which showed significant differences between the exposed and non-exposed spheroids within the reproductive-aged group.

Previous research has emphasized the detrimental effects of phthalates on ovarian function, including impaired follicle growth, oocyte fragmentation, and disrupted steroidogenesis (Niermann et al., 2015; Moyer and Hixon, 2012). Although the precise mechanisms by which phthalates influence ovarian function remain unclear, recent RNA-seq research on human ovarian stromal cells has revealed several enriched gene ontologies (GOs) related to the ECM, including regulation of ECM constituent secretion, ECM assembly and organization, ECM structural constituents, and collagen-containing ECM following phthalates treatment (Visser et al., 2024). ECM plays a crucial role in regulating ovarian function, particularly in follicle activation and oocyte maturation (Nagyová et al., 2021; Berkholtz et al., 2006). Over the past decade, the mechanobiology of the human ovary has received increasing attention, emphasizing the dynamic interplay between ovarian cells and their surrounding microenvironment (Woodruff and Shea, 2011; Thorne et al., 2015). The evidence regarding the adverse effects of phthalates on ovarian function, combined with the crucial role of ECM in folliculogenesis, led us to hypothesize that phthalates may exert their detrimental effects by disrupting ECM composition and function.

Investigating the effects of toxic substances such as PM poses significant challenges and requires careful experimental design. To address these challenges, the development of in vitro models that closely mimic the in vivo environment is essential for generating valuable insights. In this study, we utilized a 3D spheroid model that replicates the ovarian ECM (Ouni et al., 2020) to explore the toxic effects of PM. Specifically, we examined the impact of a PM on spheroids derived from cortical stromal cells of both reproductive-aged and menopausal ovaries, providing a valuable model for representation of the environmental exposures encountered by women. To our knowledge, this is the first study to investigate the toxic effects of PM on ECM components in human ovaries, with a particular focus on age-related differences.

Our primary findings revealed that PM exposure affects ECM components in the ovaries differently, depending on the reproductive stage of the ovaries. In the reproductive-aged group, PM treatment resulted in a marked increase in collagen types I and III, accompanied by a decrease in collagen VI.

Collagen type I, composed of rigid fibrils, is the most abundant collagen in the body and provides tensile strength to tissues (Hurme

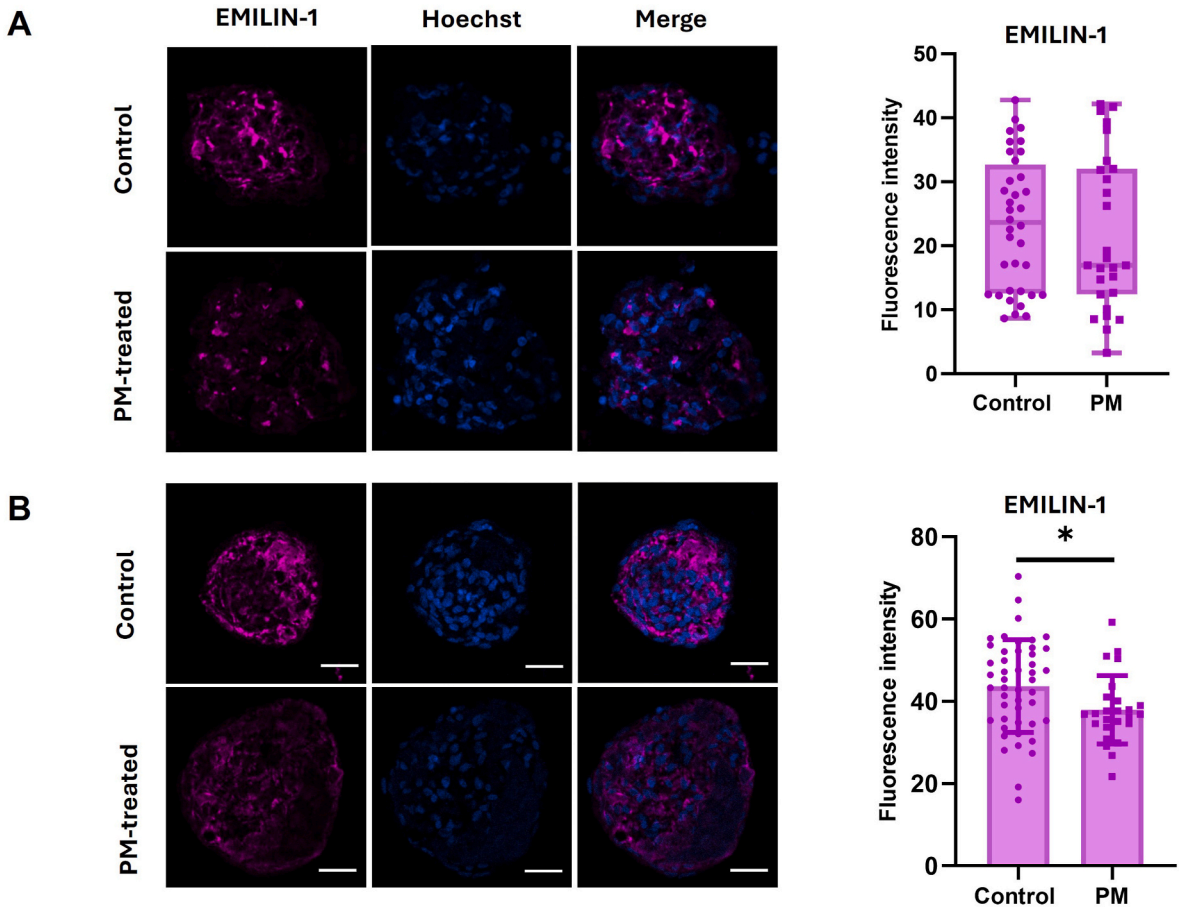

Fig. 6. EMILIN-1 immunofluorescence staining images and quantification of EMILIN-1 expression in spheroids isolated from reproductive-aged (A) and menopausal ovaries (B) exposed to PM for four days. Fluorescence intensities are presented as histograms (mean ± SEM) for normally distributed data and box plots (median ± IQR) for non-normally distributed data. A total of 135 spheroids were analyzed across all donors and treatment conditions. Each dot represents a single spheroid (technical replicate). Statistical analyses were performed using the average value per donor (biological replicate, n = 4 per group). White bars represent 25 μm * Indicates $p < 0.05$.

et al., 1991). In contrast, collagen type III, which is commonly found during the early stages of wound healing, is made up of thinner fibrils and is generally considered less mature and structurally weaker (Stadelmann et al., 1998). Evidence indicates that elevated collagen levels are linked to a shift in the ECM toward a more rigid, fibrotic state, which is closely associated with ovarian stiffness (Briley et al., 2016; Mara et al., 2020). Therefore, we hypothesize that the increase in collagen types I and III, without concurrent changes in EMILIN-1 or fibrillin-1 levels, suggests that phthalates may be driving the ECM toward a pro-fibrotic state. This shift could potentially impact ovarian function by increasing ECM stiffness. However, the lack of changes in EMILIN-1 and fibrillin-1 levels implies that the elastic properties of the ECM remain somewhat intact. Thus, the ECM may be stiffened but not yet fully fibrotic, and the tissue elasticity is likely preserved to a degree.

The observed PM-induced reduction in collagen VI in spheroids from reproductive-aged ovaries suggests that the structural and protective integrity of the ECM has been compromised. Collagen VI, the most abundant collagen type in the human ovary (Ouni et al., 2020, 2021), plays a role in protecting cells from stress and maintaining the mechanical stability of the ECM. Its reduction could lead to vulnerability of the ECM structure, making it less capable of responding to mechanical stress. Collagen VI also has cytoprotective functions, such as preventing apoptosis, reducing oxidative stress, regulating cellular differentiation, and interacting with membrane receptors (Bergé et al., 2013). Its reduction could impair cell-ECM signaling, contributing to a mechanical imbalance in the tissue even without significant changes in proliferation. While their impact on ovarian ECM remains inadequately examined, phthalates have been demonstrated to cause significant alterations in collagen levels in different tissues. Fibrosis is characterized by disrupted tissue architecture and excessive accumulation of ECM components, primarily collagen (Niermann et al., 2015). Numerous studies have investigated the role of phthalates in fibrosis development (Lee et al., 2024; Zhiwen et al., 2023), suggesting that exposure to these chemicals may contribute to pathological processes leading to fibrotic changes in diverse tissues. For instance, analysis of collagen I in human fibroid tissues implanted in mice revealed increased expression of this protein in those fed DEHP (Kim et al., 2021). Moreover, in mice exposed to PM for six months, upregulation of collagen types III and IV was observed in the uterus, with PSR staining revealing higher overall collagen levels and disorganized collagen fibers, resulting in increased uterine tissue stiffness (Shukla et al., 2023). Treatment with DEHP was also found to elevate collagen I expression in myometrial and leiomyomal cells (Kim et al., 2017) and to promote the expression of collagen I and III in the liver (Zhao et al., 2019). These findings, along with our results, emphasize the potential of phthalates to induce fibrotic and ageing-like changes in ovarian ECM, thereby impairing ovarian function.

The concentration of PM used in our study (100x) is based on the levels found in urine as phthalates undergo rapid metabolism in the body and are efficiently excreted in urine. Reliable exposure estimates are therefore often based on repeated urine sampling rather than serum, where levels fluctuate. Nevertheless, the presence of these phthalate metabolites has also been reported in ovaries and FF. For instance, higher levels of DEHP metabolites in FF, around 8 nM, have been associated with reduced steroid synthesis and a pro-inflammatory

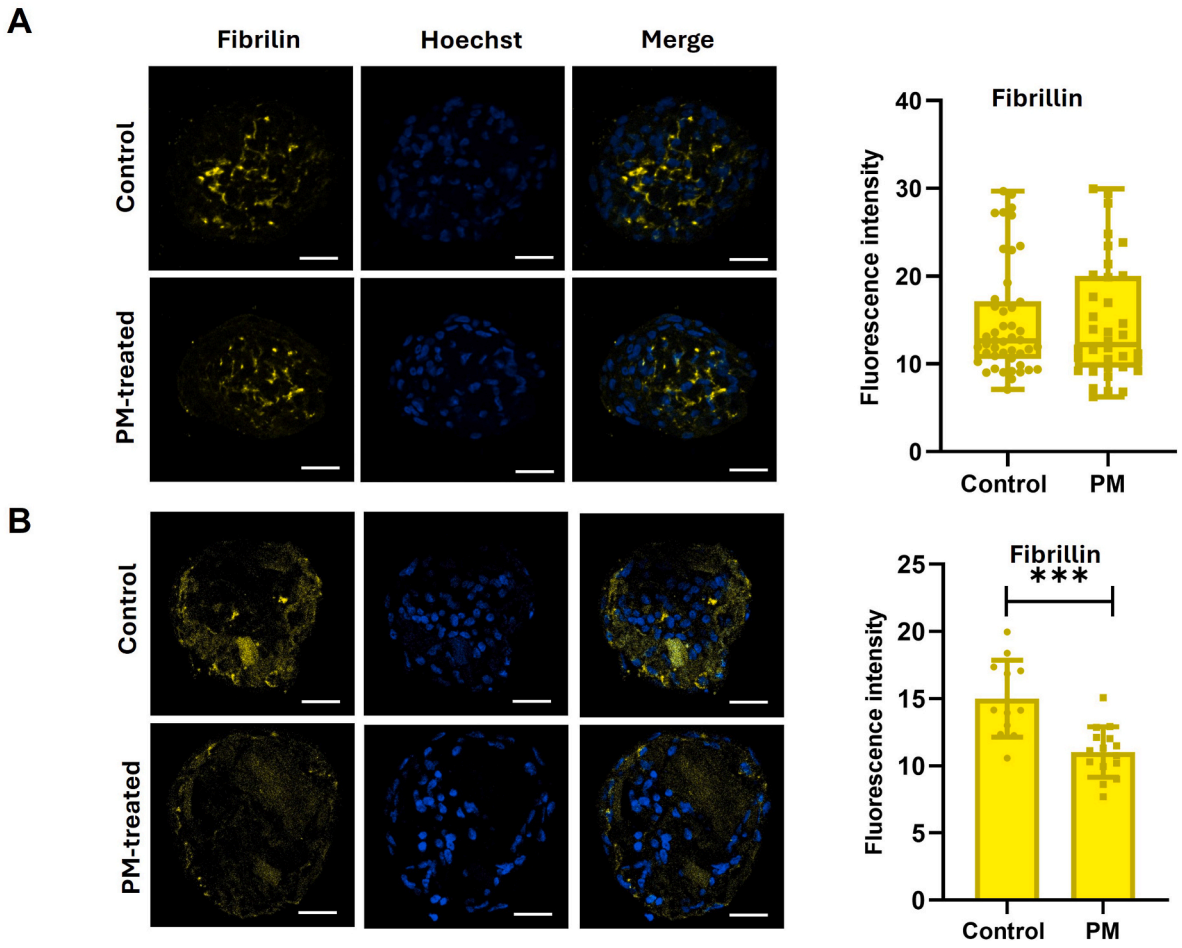

Fig. 7. Fibrillin-1 immunofluorescence staining images and quantification of fibrillin-1 expression in spheroids isolated from reproductively aged (A) and menopausal ovaries (B) exposed to PM for four days. Fluorescence intensities are presented as histograms (mean ± SEM) for normally distributed data and box plots (median ± IQR) for non-normally distributed data. A total of 109 spheroids were analyzed across all donors and treatment conditions. Each dot represents a single spheroid (technical replicate). Statistical analyses were performed using the average value per donor (biological replicate, n = 4 per group). White bars represent 25 μm *** Indicates $p < 0.001$.

environment (Varik et al., 2024). The lack of differences in spheroid size or shape may be attributed to the short duration (four days) of treatment in our study, whereas real-life exposure is lifelong and semi-persistent, meaning constant despite rapid metabolism. This observation warrants further investigation through longer-term studies.

In our study, the combined effects of increased collagen I and III and decreased collagen VI suggest that PM is promoting ECM remodeling in a way that is likely harmful to normal ovarian function. This could be due to phthalate-induced alterations in signaling pathways that regulate ECM composition, possibly through oxidative stress or altered matrix metalloproteinase (MMP) activity, which could lead to imbalanced collagen synthesis and degradation. This could have significant implications for ovarian function, particularly in folliculogenesis and oocyte maturation, as the mechanical properties of the ECM play a vital role in these processes.

Interestingly, the alterations in ECM components observed in our study differed between spheroids generated from reproductive-aged and menopausal ovaries. This variation may be attributed to different factors, such as ECM composition and functionality, hormonal status, and fibrotic nature of menopausal ovaries.

Reproductive-aged ovaries have a more dynamic and adaptable ECM that supports ongoing folliculogenesis than menopausal ovaries, which is crucial for maintaining ovarian function. The changes in collagen levels after PM exposure suggest that the ECM is actively remodeling, possibly in an attempt to repair or adapt to damage caused by the phthalates. On the other hand, in menopausal ovaries, ECM turnover is reduced, and the ECM composition has already shifted toward a more stable, fibrotic state due to natural aging processes. The absence of changes in spheroid size or collagen levels following PM exposure suggests that the ECM in menopausal ovaries may be less responsive to external damage, likely due to age-related stiffening. Since menopausal ovaries are already predisposed to fibrotic alterations, it is possible that they are already in a pro-fibrotic state. This pre-existing condition could explain why no further increases in collagen types I and III were observed after PM exposure.

The primary impact of PM exposure in spheroids from menopausal ovaries appears to target the elastic components of the ECM, as evidenced by the reduction in both EMILIN-1 and fibrillin-1 levels. These findings suggest that phthalates selectively affect key elastic components of the ECM, compromising tissue elasticity and structural integrity, even in the absence of major changes in overall ECM structure. Ouni et al. (Moyer and Hixon, 2012) previously demonstrated that fibrillin-1 availability progressively declines from prepuberty to menopause, contributing to the loss of tissue elasticity commonly associated with aging. As a result, phthalate-induced disruption of elastic components like fibrillin-1 could have significant implications for ovarian function, potentially accelerating the decline in elasticity and accelerating the onset of early menopause.

The distinct impact of phthalates on the ECM components of reproductive-aged and menopausal ovaries also highlights the influence

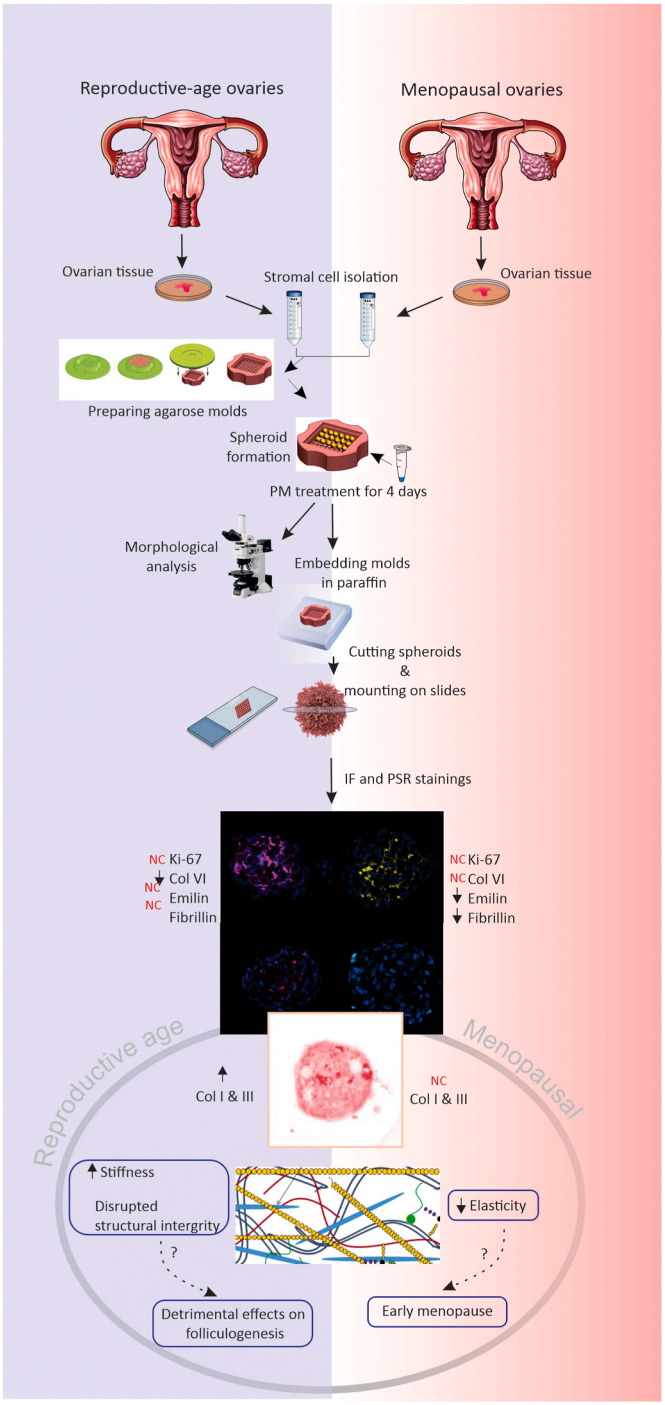

Fig. 8. Overview of the process for isolating cortical stromal cells from both reproductive age and menopausal women, forming spheroids, and treating with a phthalate mixture (PM). This figure also highlights the related analyses, including immunofluorescence (IF) and Picrosirius Red (PSR), and presents the key findings of the study. (For interpretation of the references to colour in this figure legend, the reader is referred to the Web version of this article.)

of hormonal factors on tissue response. In contrast to menopausal ovaries, the reproductive-aged ovaries are influenced by active hormonal regulation (e.g., estrogen, progesterone), which may make the ECM more sensitive to PM exposure and remodeling. Estrogen plays a crucial role in collagen cross-linking and deposition, primarily through activation of lysyl oxidase and lysyl oxidase-like 1. In addition, phthalates have been suggested to exhibit estrogenic effects (Kambia et al., 2019), and a positive association has been observed between urinary levels of DEHP and serum estradiol levels (Fong et al., 2015). Contrarily, the absence of hormonal influence in post-menopausal ovaries could reduce the ECM's responsiveness to external toxicants such as phthalates, as hormonal signals that typically regulate ECM turnover are diminished. These findings underscore the importance of understanding the interactions between phthalates and ECM, particularly in the context of aging, to better assess the risks posed by environmental toxins to reproductive health.

While our primary objective was to assess ECM remodeling in response to phthalate mixture exposure, we recognize that a deeper characterization of the spheroid cellular composition would provide additional insight into the biological context of the observed changes. Ovarian stromal tissue is inherently heterogeneous, and future studies should incorporate immunostaining or transcriptomic profiling with specific markers (e.g., for fibroblasts, endothelial cells, immune and theca cells) to better define the identity and spatial distribution of cell types within the 3D constructs. Similarly, including markers of apoptosis or necrosis would complement the proliferation data and contribute to a more comprehensive understanding of spheroid viability under toxicant exposure.

In addition, while the use of DMSO-matched controls ensured that PM-specific effects could be discerned, the absence of a medium-only group limits our ability to fully assess potential DMSO-related effects on spheroid behavior. Future experimental designs should incorporate both vehicle and untreated controls to strengthen mechanistic interpretation.

Finally, we note that staining and imaging for reproductive-age and menopausal cohorts were performed independently, precluding direct quantitative comparisons between age groups. Although this design allowed us to focus on intra-group responses to PM exposure, future studies would benefit from harmonized processing to enable robust cross-cohort analyses and further explore age-related ECM changes.

5. Conclusion

In this study, we demonstrated that PM exposure had distinct, reproductive stage-specific effects on ECM composition in ovarian spheroids. In spheroids derived from reproductive-aged ovaries, PM exposure led to increased collagen deposition, potentially disrupting the delicate ECM balance, which is essential for normal ovarian function and cyclic remodeling. Conversely, after PM treatment, spheroids from menopausal ovaries exhibited a reduction in EMILIN-1 and fibrillin-1, key proteins essential for maintaining tissue elasticity, highlighting a different vulnerability in aging ovarian tissue. These findings underscore the utility of 3D spheroid models as reliable in vitro tools for investigating the impact of toxicants on ovarian function, allowing for the study of tissue structure and function in a controlled environment. Additionally, spheroids offer significant advantages by reducing reliance on animal models while providing a more accurate representation of human tissue architecture, paving the way for more ethical and relevant toxicological research.

CRediT authorship contribution statement

Saba Nikanfar: Writing – original draft, Visualization, Validation, Software, Methodology, Investigation, Data curation. **Ellen C.R. Leonel:** Writing – review & editing, Validation, Investigation, Data curation, Conceptualization. **Pauliina Damdimopoulou:** Writing – review & editing, Validation, Resources, Methodology, Funding acquisition. **Jodi A. Flaws:** Writing – review & editing, Validation, Resources, Methodology, Funding acquisition. **Christiani A. Amorim:** Writing – review & editing, Validation, Supervision, Resources, Project administration, Funding acquisition, Conceptualization.

Funding statement

This study was supported by the Fonds National de la Recherche Scientifique de Belgique (FNRS-CDR Convention grant number J.0004.21) and Fédération Wallonie-Bruxelles (WBI SUB/2022/566002) awarded to C.A.A., FSR Incoming Post-doc Fellowship (grant number: IRECFSR23MOVEAND) awarded to S.N., NIEHS R01 ES034112 awarded to J.A.F., Swedish Research Council for Sustainable Development FORMAS (2018-02280), and Goiás State Research Support Foundation (grant FAPEG 202310267000338) awarded to E.C.R.L.

Declaration of competing interest

The authors declare the following financial interests/personal relationships which may be considered as potential competing interests: Christiani A. Amorim reports a relationship with Fund for Scientific Research that includes: funding grants. Christiani A. Amorim reports a relationship with Federation of Wallonia and Brussels that includes: funding grants. Saba Nikanfar reports a relationship with Fonds spécial de recherche that includes: funding grants. Jody Flaws reports a relationship with National Institute of Environmental Health Sciences that includes: funding grants. Pauliina Damdimopoulou reports a relationship with Swedish Research Council Formas that includes: funding grants. Ellen Leonel reports a relationship with Foundation for Research Support of Goiás State that includes: funding grants. If there are other authors, they declare that they have no known competing financial interests or personal relationships that could have appeared to influence the work reported in this paper.

Acknowledgements

We sincerely thank the Transplantation Unit of UCLouvain's Saint-Luc Hospital for their invaluable contribution to this study through the donation of ovarian tissue.

Appendix A. Supplementary data

Supplementary data to this article can be found online at https://doi.org/10.1016/j.envres.2025.121797.

Data availability

Data will be made available on request.

References

Adir, M., Salmon-Divon, M., Combelles, C.M.H., Mansur, A., Cohen, Y., Machtinger, R., 2017. In vitro exposure of human luteinized mural granulosa cells to dibutyl phthalate affects global gene expression. Toxicol. Sci. : J. Off. Soc. Toxicol. 160 (1), 180–188.

Barnett-Itzhaki, Z., Knapp, S., Avraham, C., Racowsky, C., Hauser, R., Bollati, V., et al., 2021. Association between follicular fluid phthalate concentrations and extracellular vesicle microRNAs expression. Hum. Reprod. 36 (6), 1590–1599.

Bellavia, A., Zou, R., Björvang, R.D., Roos, K., Sjunnesson, Y., Hallberg, I., et al., 2023. Association between chemical mixtures and female fertility in women undergoing assisted reproduction in Sweden and Estonia. Environ. Res. 216 (Pt 1), 114447.

Bergé, A., Cladière, M., Gasperi, J., Coursimault, A., Tassin, B., Moilleron, R., 2013. Meta-analysis of environmental contamination by phthalates. Environ. Sci. Pollut. Res. Int. 20 (11), 8057–8076.

Berkholtz, C.B., Shea, L.D., Woodruff, T.K., 2006. Extracellular matrix functions in follicle maturation. Semin. Reprod. Med. 24 (4), 262–269.

Briley, S.M., Jasti, S., McCracken, J.M., Hornick, J.E., Fegley, B., Pritchard, M.T., et al., 2016. Reproductive age-associated fibrosis in the stroma of the mammalian ovary. Reproduction 152 (3), 245–260.

Chang, Y.J., Tseng, C.Y., Lin, P.Y., Chuang, Y.C., Chao, M.W., 2017. Acute exposure to DEHP metabolite, MEHP cause genotoxicity, mutagenesis and carcinogenicity in mammalian Chinese hamster ovary cells. Carcinogenesis 38 (3), 336–345.

Chen, H.S., Chiang, P.H., Wang, Y.C., Kao, M.C., Shieh, T.H., Tsai, C.F., et al., 2012. Benzyl butyl phthalate induces necrosis by AhR mediation of CYP1B1 expression in human granulosa cells. Reprod. Toxicol. 33 (1), 67–75.

Chiti, M.C., Dolmans, M.M., Hobeika, M., Cernogoraz, A., Donnez, J., Amorim, C.A., 2017. A modified and tailored human follicle isolation procedure improves follicle recovery and survival. J. Ovarian Res. 10 (1), 71.

Dipali, S.S., King, C.D., Rose, J.P., Burdette, J.E., Campisi, J., Schilling, B., et al., 2023. Proteomic quantification of native and ECM-enriched mouse ovaries reveals an age-dependent fibro-inflammatory signature. Aging. 15 (20), 10821–10855.

Du, Y.Y., Fang, Y.L., Wang, Y.X., Zeng, Q., Guo, N., Zhao, H., et al., 2016. Follicular fluid and urinary concentrations of phthalate metabolites among infertile women and associations with in vitro fertilization parameters. Reprod. Toxicol. 61, 142–150.

Evangelinakis, N., Geladari, E.V., Geladari, C.V., Kontogeorgi, A., Papaioannou, G.K., Peppa, M., et al., 2024. The influence of environmental factors on premature ovarian insufficiency and ovarian aging. Maturitas 179, 107871.

Fong, J.P., Lee, F.J., Lu, I.S., Uang, S.N., Lee, C.C., 2015. Relationship between urinary concentrations of di(2-ethylhexyl) phthalate (DEHP) metabolites and reproductive hormones in polyvinyl chloride production workers. Occup. Environ. Med. 72 (5), 346–353.

Gallardo, M., Paulini, F., Corral, A., Balcerzyk, M., Lucci, C.M., Ambroise, J., et al., 2018. Evaluation of a new freezing protocol containing 20% dimethyl sulphoxide concentration to cryopreserve human ovarian tissue. Reprod. Biomed. Online 37 (6), 653–665.

Gonsioroski, A.V., Aquino, A.M., Alonso-Costa, L.G., Barbisan, L.F., Scarano, W.R., Flaws, J.A., 2022. Multigenerational effects of an environmentally relevant phthalate mixture on reproductive parameters and ovarian miRNA expression in female rats. Toxicol. Sci. : J. Off. Soc. Toxicol. 189 (1), 91–106.

Hong, Y., Wu, S., Wei, G., 2023. Adverse effects of microplastics and nanoplastics on the reproductive system: a comprehensive review of fertility and potential harmful interactions. Sci. Total Environ. 903, 166258.

Hongjun, Y., Wenjun, X., Qing, L., Jingtao, L., Hongwen, Y., Zhaohua, L., 2013. Distribution of phthalate esters in topsoil: a case study in the Yellow River Delta, China. Environ. Monit. Assess. 185 (10), 8489–8500.

Hurme, T., Kalimo, H., Sandberg, M., Lehto, M., Vuorio, E., 1991. Localization of type I and III collagen and fibronectin production in injured gastrocnemius muscle. Lab. Invest. J. Tech. Methods Pathol. 64 (1), 76–84.

Kambia, N.K., Séverin, I., Farce, A., Moreau, E., Dahbi, L., Duval, C., et al., 2019. In vitro and in silico hormonal activity studies of di-(2-ethylhexyl)terephthalate, a di-(2-ethylhexyl)phthalate substitute used in medical devices, and its metabolites. J. Appl. Toxicol. : JAT. 39 (7), 1043–1056.

Kavlock, R., Boekelheide, K., Chapin, R., Cunningham, M., Faustman, E., Foster, P., et al., 2002. NTP center for the evaluation of risks to human reproduction: phthalates expert panel report on the reproductive and developmental toxicity of di(2-ethylhexyl) phthalate. Reprod. Toxicol. 16 (5), 529–653.

Kim, J.H., Kim, S.H., Oh, Y.S., Ihm, H.J., Chae, H.D., Kim, C.H., et al., 2017. In vitro effects of phthalate esters in human myometrial and leiomyoma cells and increased urinary level of phthalate metabolite in women with uterine leiomyoma. Fertil. Steril. 107 (4), 1061, 9.e1.

Kim, H.J., Kim, S.H., Oh, Y.S., Heo, S.H., Kim, K.H., Kim, D.Y., et al., 2021. Effects of phthalate esters on human myometrial and fibroid cells: cell culture and NOD-SCID mouse data. Reprod. Sci. 28 (2), 479–487.

Krotz, S.P., Carson, S.A., Tomey, C., Buster, J.E., 2012. Phthalates and bisphenol do not accumulate in human follicular fluid. J. Assist. Reprod. Genet. 29 (8), 773–777.

Land, K.L., Lane, M.E., Fugate, A.C., Hannon, P.R., 2021. Ovulation is inhibited by an environmentally relevant phthalate mixture in mouse antral follicles in vitro. Toxicol. Sci. : J. Off. Soc. Toxicol. 179 (2), 195–205.

Lee, J., Chang, S.H., Cho, Y.H., Kim, J.S., Kim, H., Zaheer, J., et al., 2024. Prenatal to peripubertal exposure to Di(2-ethylhexyl) phthalate induced endometrial atrophy and fibrosis in female mice. Ecotoxicol. Environ. Saf. 269, 115798.

Mara, J.N., Zhou, L.T., Larmore, M., Johnson, B., Ayiku, R., Amargant, F., et al., 2020. Ovulation and ovarian wound healing are impaired with advanced reproductive age. Aging 12 (10), 9686–9713.

Martine, B., Marie-Jeanne, T., Cendrine, D., Fabrice, A., Marc, C., 2013. Assessment of adult human exposure to phthalate esters in the urban centre of Paris (France). Bull. Environ. Contam. Toxicol. 90 (1), 91–96.

Mattson, E., Warner, G.R., 2025. Single cell RNA-seq reveals that granulosa cells are a target of phthalate toxicity in the ovary. Toxicol. Sci. 204, 169-180.

Meling, D.D., Warner, G.R., Szumski, J.R., Gao, L., Gonsioroski, A.V., Rattan, S., et al., 2020. The effects of a phthalate metabolite mixture on antral follicle growth and sex steroid synthesis in mice. Toxicol. Appl. Pharmacol. 388, 114875.

Moyer, B., Hixon, M.L., 2012. Reproductive effects in F1 adult females exposed in utero to moderate to high doses of mono-2-ethylhexylphthalate (MEHP). Reprod. Toxicol. 34 (1), 43–50.

Nagyová, E., Němcová, L., Camaioni, A., 2021. Cumulus extracellular matrix is an important part of oocyte microenvironment in ovarian follicles: its remodeling and proteolytic degradation. Int. J. Mol. Sci. 23 (1).

Niermann, S., Rattan, S., Brehm, E., Flaws, J.A., 2015. Prenatal exposure to di-(2-ethylhexyl) phthalate (DEHP) affects reproductive outcomes in female mice. Reprod. Toxicol. 53, 23–32.

Ouni, E., Bouzin, C., Dolmans, M.M., Marbaix, E., Pyr Dit Ruys, S., Vertommen, D., et al., 2020. Spatiotemporal changes in mechanical matrisome components of the human ovary from prepuberty to menopause. Hum. Reprod. 35 (6), 1391–1410.

Ouni, E., Peaucelle, A., Haas, K.T., Van Kerk, O., Dolmans, M.M., Tuuri, T., et al., 2021. A blueprint of the topology and mechanics of the human ovary for next-generation bioengineering and diagnosis. Nat. Commun. 12 (1), 5603.

Rasmussen, L.M., Sen, N., Vera, J.C., Liu, X., Craig, Z.R., 2017. Effects of in vitro exposure to dibutyl phthalate, mono-butyl phthalate, and acetyl tributyl citrate on ovarian antral follicle growth and viability. Biol. Reprod. 96 (5), 1105–1117.

Repouskou, A., Panagiotidou, E., Panagopoulou, L., Bisting, P.L., Tuck, A.R., Sjödin, M.O. D., et al., 2019. Gestational exposure to an epidemiologically defined mixture of phthalates leads to gonadal dysfunction in mouse offspring of both sexes. Sci. Rep. 9 (1), 6424.

Safar, A.M., Santacruz-Márquez, R., Laws, M.J., Meling, D.D., Liu, Z., Kumar, T.R., et al., 2023. Dietary exposure to an environmentally relevant phthalate mixture alters follicle dynamics, hormone levels, ovarian gene expression, and pituitary gene expression in female mice. Reprod. Toxicol. 122, 108489.

Shukla, R., Arshee, M.R., Laws, M.J., Flaws, J.A., Bagchi, M.K., Johnson, A.J.W., et al., 2023. Chronic exposure of mice to phthalates enhances TGF beta signaling and promotes uterine fibrosis. Reprod. Toxicol. 122, 108491.

Stadelmann, W.K., Digenis, A.G., Tobin, G.R., 1998. Physiology and healing dynamics of chronic cutaneous wounds. Am. J. Surg. 176 (2A Suppl. l), 26s–38s.

Tarvainen, I., Soto, D.A., Laws, M.J., Björvang, R.D., Damdimopoulos, A., Roos, K., et al., 2023. Identification of phthalate mixture exposure targets in the human and mouse ovary in vitro. Reprod. Toxicol. 119, 108393.

Thorne, J.T., Segal, T.R., Chang, S., Jorge, S., Segars, J.H., Leppert, P.C., 2015. Dynamic reciprocity between cells and their microenvironment in reproduction. Biol. Reprod. 92 (1), 25.

Varik, I., Zou, R., Bellavia, A., Rosenberg, K., Sjunnesson, Y., Hallberg, I., et al., 2024. Reduced ovarian cholesterol and steroid biosynthesis along with increased inflammation are associated with high DEHP metabolite levels in human ovarian follicular fluids. Environ. Int. 191, 108960.

Visser, N., Silva, A.V., Tarvainen, I., Damdimopoulos, A., Davey, E., Roos, K., et al., 2024. Epidemiologically relevant phthalates affect human endometrial cells in vitro through cell specific gene expression changes related to the cytoskeleton and mitochondria. Reprod. Toxicol. 128, 108660.

Woodruff, T.K., Shea, L.D., 2011. A new hypothesis regarding ovarian follicle development: ovarian rigidity as a regulator of selection and health. J. Assist. Reprod. Genet. 28 (1), 3–6.

Zhang, M., Liu, C., Yuan, X.Q., Cui, F.P., Miao, Y., Yao, W., et al., 2023. Individual and joint associations of urinary phthalate metabolites with polycystic ovary and polycystic ovary syndrome: results from the TREE cohort. Environ. Toxicol. Pharmacol. 102, 104233.

Zhao, Z.B., Ji, K., Shen, X.Y., Zhang, W.W., Wang, R., Xu, W.P., et al., 2019. Di(2-ethylhexyl) phthalate promotes hepatic fibrosis by regulation of oxidative stress and inflammation responses in rats. Environ. Toxicol. Pharmacol. 68, 109–119.

Zhiwen, X., Yongqing, Z., Wenlan, S., Shan, H., Bangmin, H., Juntao, J., et al., 2023. Dibutyl phthalate induces epithelial-mesenchymal transition of renal tubular epithelial cells via the Ang II/AMPKα2/Cx43 signaling pathway. Toxicology 494, 153584.

Zhou, C., Flaws, J.A., 2017. Effects of an environmentally relevant phthalate mixture on cultured mouse antral follicles. Toxicol. Sci. : J. Off. Soc. Toxicol. 156 (1), 217–229.